Manifestations of geometrical and dynamical phases for the photon under cyclic and non-cyclic evolutions

M. GRETHER G., E. LÓPEZ-MORENO

Departamento de Física, Facultad de Ciencias
Universidad Nacional Autónoma de México
04510 México, D.F., México

AND

A. GÓNGORA T.

Instituto de Física, Universidad Nacional Autónoma de México
04510 México, D.F., México

ABSTRACT. We review the geometrical phases in a non planar Mach-Zehnder interferometer as a non adiabatic Aharonov-Anandan phase shift. Light traveled interferometer's arms along paths twisted in the three spatial dimensions. Both arms were arranged symmetrically, having opposite senses of handedness. By considering the light at the asymmetrical second exit of the interferometer, we prove that the process *needs not* to be cyclic to exhibit geometrical phases. We also prove that a purely dynamical phase shift does not affect the relative fringe shifts associated with geometrical phases. The method of distinguishing geometrical and dynamical phases is to perform the same experiment with opposite helicities.

RESUMEN. Presentamos una revisión de las fases geométricas dentro de un interferómetro Mach-Zehnder no-plano contempladas como desfases no-adiabáticos del tipo Aharonov-Anandan. La luz recorrió los brazos del interferómetro en caminos que incluyen torceduras dirigidas en las tres dimensiones del espacio. Los brazos fueron dispuestos simétricamente, con sentidos opuestos en su simetría izquierda-derecha. Considerando la luz en la salida asimétrica del interferómetro, probamos que el proceso *no necesita* ser cíclico para exhibir fases geométricas. También probamos que un desfase puramente dinámico no afecta los corrimientos relativos de las franjas asociados con las fases geométricas. El método de distinguir las fases geométricas de las dinámicas consistió en realizar el mismo experimento con helicidades opuestas.

1. INTRODUCTION

Some years ago, Berry [1] made a very important prediction concerning the phase of eigenvectors of any system in wave physics: A physical system acquires, with a cyclic adiabatical evolution, not only a dynamical phase factor, but also another phase factor not associated with time evolution of the system. This Berry's phase, also called the geometrical phase, represents, under continuation of the cycle of evolution, a non-integrable phase factor which is associated with the geometrical aspects of the evolution of the system. In his original work, Berry deals with the quantum adiabatic theorem and considers non-degenerate eigenstates of a quantum mechanical system transported adiabatically around

a closed path C in the space of parameters on which the Hamiltonian depends. Some years later, Aharonov and Anandan [2] gave a generalization of Berry's phase including non-adiabatical processes. Instead of the Hamiltonian in a parameter space, they deal with the state vector describing the physical system in that case on which this vector carries out a cyclic evolution. They gave a formula in terms of the circuits that the state vector projects in a projective Hilbert space, rather than adiabatic circuits of the Hamiltonian itself in the parameter space. Samuel and Bhandari [3] later proved that even the cyclic hypothesis could be relaxed.

In optics, geometrical effects have been observed in the phase of light in two different kinds of experiments. A first kind involves evolutions in the polarization state of light [4]. As it is well known [5], each polarization state can be associated with a projected point on the Poincarè sphere. With a cyclic evolution in the polarization state, we shall get a closed circuit C on that sphere. Here, geometrical phase depends on *the solid semi angle* subtended by circuit C at the center of this sphere. This is Pancharatnam phase factor in the context of optics [6]. A second kind of experiments involves rotations and inversions of photon spin in tridimensional space. In this second case, the geometrical phase depends on *the solid angle* subtended by circuit C described by the projection of photon spin on the unitary sphere of all possible directions of the photon propagation vector $\mathbf{k}$. This projective circuit C can be accomplished in any coiled light experiment [7].

Phase factors are observable by interference if a cycled system is recombined with another reference system. In our experiment the two light beams, one for each arm of an interferometer, constitute the two systems. Any extra phase shift between both systems, either dynamical or geometrical, manifests itself experimentally as a fringe displacement in the observed interference pattern. Therefore, it is of fundamental importance to ensure that the fringe displacements observed can be identified with changes in geometrical phase. The only one physical observable is light intensity in the interference fringe pattern. Photons with positive helicity $|+\rangle$ do not interfere with those of negative helicity $|-\rangle$, because they are in mutually orthogonal polarized states. Each of those helicity states produce their own interference pattern. In a non-polarized light beam we have $|+\rangle$ and $|-\rangle$ photons randomly mixed. The observed intensity of such a beam, after passing the interferometer, is the addition of the intensities of the two interference patterns projected, namely, on an observation screen. Dynamical phase shift, related with optical path length, results the same for both kinds of photons through a given interferometer's arm. The purpose of the present paper is to review the experimental effects of geometrical phase in contrast with the dynamical phase in an optical non-planar Mach-Zehnder interferometer as the one used by Chiao *et al.* [8] (Fig. 1). We show that geometrical phase is observed in an independent way of the dynamical phase shifts. In optics this is not a generally valid assertion; in fact, in those experiments associated with Pancharatnam phase [6] it is not possible to tell if the fringe advance is a result of a geometrical or of a dynamical phase shift. In this experiment we also prove that the process needs not to be cyclic to get a geometrical phase shift.
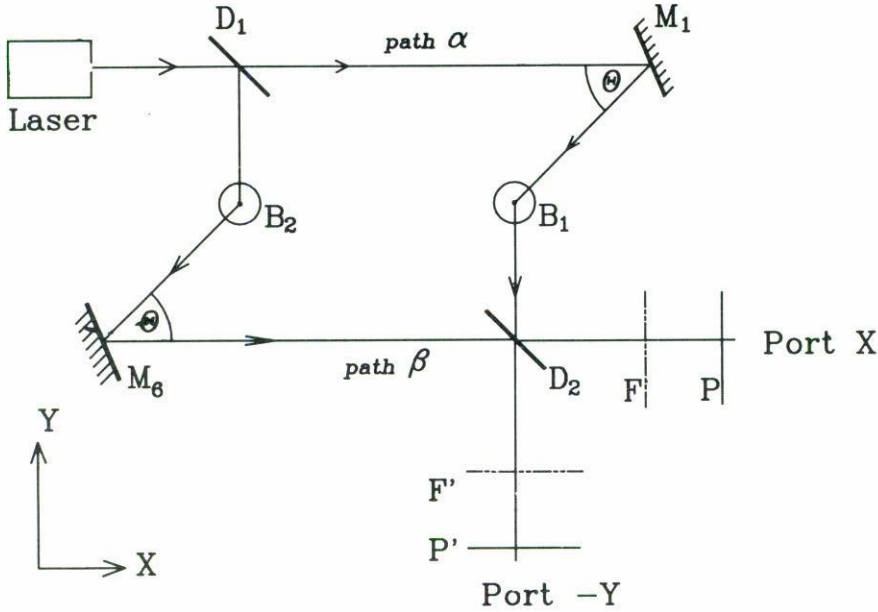
FIGURE 1. Mach-Zehnder interferometer. The upper half of the diagram are at a lower height from the lower half of the diagram by 8 cm. B_1 and B_2 are beam elevators. Mirrors M_2, M_3 are in B_1 and mirrors M_4, M_5 are in B_2. The distance from D_1 to the lower mirror (M_4) in B_2 is 20 cm. D_1 and M_1 are 37 cm apart. F and F' are the polarization filter planes. P and P' are the observation planes. Focusing optics is located between F and P; and between F' and P'.

2. DISCUSSION

Photons are massless spin-1 bosons. They have helicity $\mathbf{s} \cdot \mathbf{k}$, where $\mathbf{s}$ is the spin operator and $\mathbf{k}$ is the direction of propagation. Zero rest mass of the photon guarantees that its helicity will remain either $+1$ or -1. Inside the nonplanar Mach-Zehnder interferometer (Fig. 1) the optical path length is related to the usual dynamical phase acquired by the photon through interferometer's arms. We suppose for the moment, ideally, that optical path lengths of both arms are exactly the same all along the experiment. The spinning photon changes its direction upon reflection in each mirror and also (with perfectly conducting surfaces) reverses its helicity; it does not changes upon transmission through a metallic beam splitter. For each photon, within a given interferometer's arm (α or β in Fig. 1), we get a curve $\mathcal{C}$ projected by the spin eigenstate on a unit sphere Σ of all directions in the three dimensional configuration space. (See Figs. 2a and 2b). Circuit $\mathcal{C}_{\alpha+}$ is the result of projecting the $|+\rangle$ eigenstate of photon spin over the sphere Σ as this photon propagates along the α arm of the interferometer. The photon $|+\rangle$ enters to the interferometer along the X-axis and the projection of its spin falls in point A on Σ (Fig. 2a). Upon transmission through D_1, photon's direction remains along the X-axis and A is still the projection point on Σ. Under reflection on mirror M_1 the photon changes both, helicity and direction; it travels in direction of the vector $(-\cos\Theta, -\sin\Theta, 0)$ and, because of reflection, point B in Fig. 2a results the new spin projection point on Σ, whose coordinates are: $(\cos\Theta, \sin\Theta, 0)$. Then, the photon travels from mirror M_1 to beam
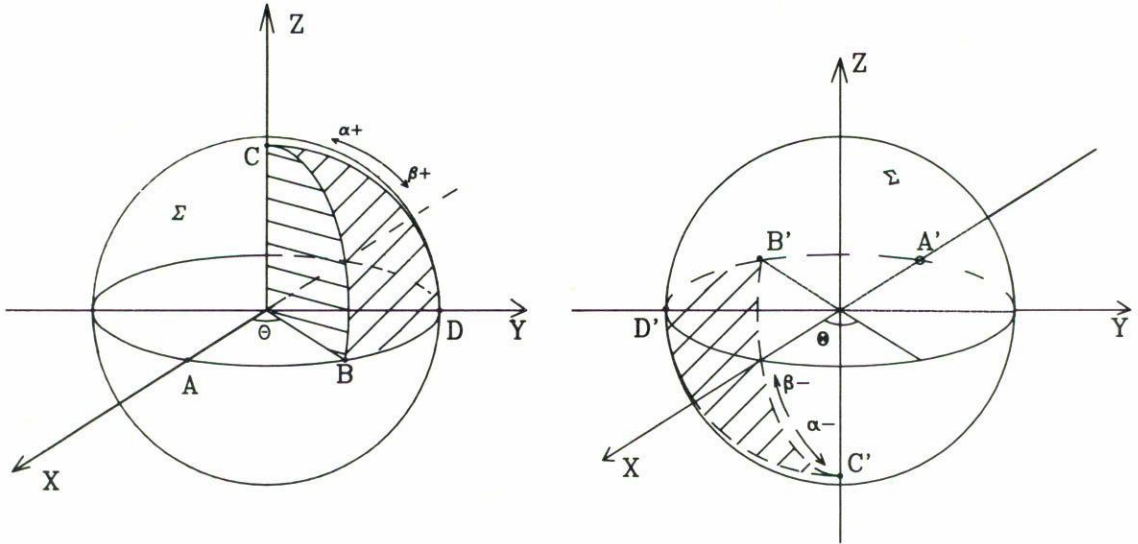
FIGURE 2. a) Unitary sphere Σ of spin directions of the photon for the two arms $(i = \alpha, \beta)$ of the interferometer. Hatching represents the absolute value of the solid angle $|\Omega(\mathcal{C}_{i,+})|$ for the photon $|+\rangle$. b) Unitary sphere Σ of spin directions of the photon for the two arms $(i = \alpha, \beta)$ of the interferometer. Hatching represents the absolute value of the solid angle $|\Omega(\mathcal{C}_{i,-})|$ for the photon $|-\rangle$.

elevator B_1, which contains the two mirrors M_2 (lower) and M_3 (higher). The photon goes from M_2 to M_3. After reflection on mirror M_2, the photon travels in the direction of the Z-axis and the spin projection on Σ changes to point C: $(0, 0, 1)$ on Σ (Fig. 2a). The mirror M_3 reflects the photon in the negative direction of the Y-axis, but the projection of the spin is over the point D: $(0, 1, 0)$ on Σ (Fig. 2a). Finally, the beam splitter D_2 reflects the photon over its original direction of propagation, closing the circuit on Σ by passing through B, as the spin projection goes from D to A. Thus, the closed circuit $\mathcal{C}_{\alpha+}$ will be formed by the projection points $ABCDA$, which subtends the spherical triangle BCD. In the above paragraph we have taken into account that each reflection changes the helicity of the photon with a probability $P_{+-} = 1$ (for silver, $P_{+-} = 0.958$ [7]). Let us consider the circuit $\mathcal{C}_{\beta+}$ corresponding to the photon $|+\rangle$ propagating through the arm β of the interferometer. It is constructed in an analogous form to that of the previous case, resulting on the closed circuit on Σ: $ADCBA$, subtending the same spherical triangle BCD on Σ, but in this case the path is travelled on opposite sense to that corresponding to $\mathcal{C}_{\alpha+}$ (Fig. 2a). Let us consider now circuits $\mathcal{C}_{\alpha-}$ and $\mathcal{C}_{\beta-}$, corresponding to photon $|-\rangle$. Both are projected on the same spherical triangle $B'C'D'$ as is shown in Fig. 2b. They are obtained through a similar process as the one described previously. They also result running in opposite senses with respect to each other; triangle $B'C'D'$ belongs to $\mathcal{C}_{\alpha-}$ and triangle $B'D'C'$ to $\mathcal{C}_{\beta-}$.

Let Ω be ‘he solid angle that any of those circuits $\mathcal{C}$ subtends at the center of sphere

Σ. In order to define circuit $\mathcal{C}$ we had joined discrete spin directions by great circles [3]. $\mathcal{C}$ represents a cyclic evolution of the spin state vector of the photon which acquires, after a complete cycle, an Aharonov-Anandan phase:

$$\gamma_{i\sigma} = \Omega(\mathcal{C}_{i\sigma}), \qquad i = \alpha, \beta: \quad \sigma = +, -; \tag{1}$$

where σ is the helicity of the photon. Equation (1) differs from Eq. (1) in Ref. [8] in that it is free from the context of adiabatic evolutions of a Hamiltonian and does not contain the factor $-\sigma$, which arises from the "interaction Hamiltonian $\mathbf{s} \cdot \mathbf{k}$" (see Eqs. (1-5), in Chiao and Wu, Ref. [7]). Indeed, we obtain this geometrical phase in the context of the Aharonov-Anandan theory [2]. For example, in Ref. [2], for an 1/2 spin particle with a magnetic moment inside an homogeneous magnetic field $\mathbf{B}$ along Z-axis, we know that it acquires a geometrical phase equal to *the absolute value of the spin times the solid angle subtended by a curve traced on the sphere* Σ (defined above) *by the direction of the spin state at the center.* Notably, in this theory the geometrical phase *does not* depend on neither the Hamiltonian, nor on the dynamical phase or the parameter used to trace $\mathcal{C}$; it depends *only* on the geometry of curve $\mathcal{C}$. We take a unitary spin for the photon and Eq. (1) implies a sign convention for $\Omega(\mathcal{C})$: $\mathcal{C}$ has an orientation given by the sense of circulation around it. We shall have $\Omega(\mathcal{C}) > 0$ if the orientation of $\mathcal{C}$ points *outwards* from Σ, in accord to the right-hand rule. Figs. 2a and 2b resume the four possible circuits $\mathcal{C}_{i\sigma}$, holding for each arm (subscript i) and a given initial helicity (subscript σ) of the photon in the interferometer.

Now we consider the relationship between the solid angle $\Omega(\mathcal{C}_{i\sigma})$, mentioned above, and the angle Θ involved in the geometry of the configuration of the interferometer's arms (Fig. 1). In each case curve $\mathcal{C}_{i\sigma}$ traces an spherical triangle with two of their vertices on the equator and a third on a pole (Figs. 2a and 2b). According to Gauss-Bonnet theorem, the sum of internal angles in a spherical triangle equals to $\pi + \Omega(\mathcal{C}_{i\sigma})$, and then we can find for our $\mathcal{C}_{i\sigma}$:

$$|\Omega(\mathcal{C}_{i\sigma})| = (\frac{\pi}{2} - \Theta), \tag{2}$$

where $0 < \Theta < \pi/2$. For each interferometer's arm and a given initial helicity of the photon, Table I shows geometrical phases acquired by this photon.

TABLE I.

$\gamma_{i}{}^{\sigma}$	$(+)$	$(-)$
α	$-(\pi/2-\Theta)$	$(\pi/2-\Theta)$
β	$(\pi/2-\Theta)$	$-(\pi/2-\Theta)$

Therefore a photon acquires an additional phase factor $\gamma_{i\sigma}$ which does not exists in a conventional planar interferometer. At the exit of the non-planar interferometer geometrical phase differences between photons of identical helicity states are, according to Table I:

$$\Delta\gamma_+ = -(\pi - 2\Theta), \qquad \Delta\gamma_- = +(\pi - 2\Theta); \tag{3}$$

where we write $\Delta\gamma_+ \equiv \gamma_{\alpha+} - \gamma_{\beta+}$ and $\Delta\gamma_- \equiv \gamma_{\alpha-} - \gamma_{\beta-}$.

In a bidimensional interferometer interference patterns of light with circular polarization of opposite helicity states share identical positions on observation screen. In contrast, in a tridimensional one both patterns are shifted according to their geometrical phase shifts $\Delta\gamma_+$ and $\Delta\gamma_-$, respectively. These shifts are of the same magnitude, but of opposite directions on the screen. Any further dynamical phase shifts, whatsoever, not only will be independent of this geometrical phase but, in this kind of optical experiments, will also be clearly discernible (unlike those in which Poincarè sphere is taken as the projective space). Here, if each circuit $\mathcal{C}_{i\sigma}$ on Σ remains invariant, we can introduce a measurable dynamical phase shift and, nevertheless, keep the geometrical shifts in Eq. (3) invariant and discernible along the experiment. We introduce an additional dynamical phase shift by means of the addition an optical window (Ealing, mod. 35-9125) in only one arm of the interferometer. All this is illustrated in Figs. 3a-3d and 4a-4d.

3. THE EXPERIMENT

The apparatus employed in our experiment consist essentially of a randomly polarized laser source light, a Mach-Zehnder interferometer with its two arms twisted in tridimensional space and having opposite handedness, a vibration isolation system, circular polarization filters and a lens device to project the interferogram on a detection screen or, alternatively, on the film in a photographic camera (Fig. 1).

A 10 mW light beam from a He-Ne non-polarized laser (NEC, mod. GLG-5261), points in the X-axis direction (see Fig. 1) and enters to the interferometer. Inside the interferometer, the light beam is divided by means of non-polarizing beam splitting cubes D_1 and D_2 (Oriel, mod. 46170). A photon incident on one of this beam splitters has the same probability amplitude of being transmitted or reflected. The two beam elevators are provided with a vibration damping design (Oriel, mod. 66421). Mirrors M_1 to M_6 are aluminized-front-surface precision flat reflectors (Oriel, mods. 44130 and 44150). All optical components of the interferometer were mounted and carefully bolted down onto an optical breadboard (Ealing, mod. 37-8299) which rests in a vibration isolation system (Ealing, U-Frame mod. 22-6670, plus a 90 kg steel ballast plate). This accomplishes the required mechanical stability for fringe measurements. The detection device was mounted apart from isolation system at the symmetric (asymmetric) exit of the interferometer. It consist of an optical bench aligned on X-axis (Y-axis), a traveling micrometer eyepiece, with a plain crossline reticle affixed to it (Ealing, mod. 11-5162) and a final plane with a screen or a photographic film.
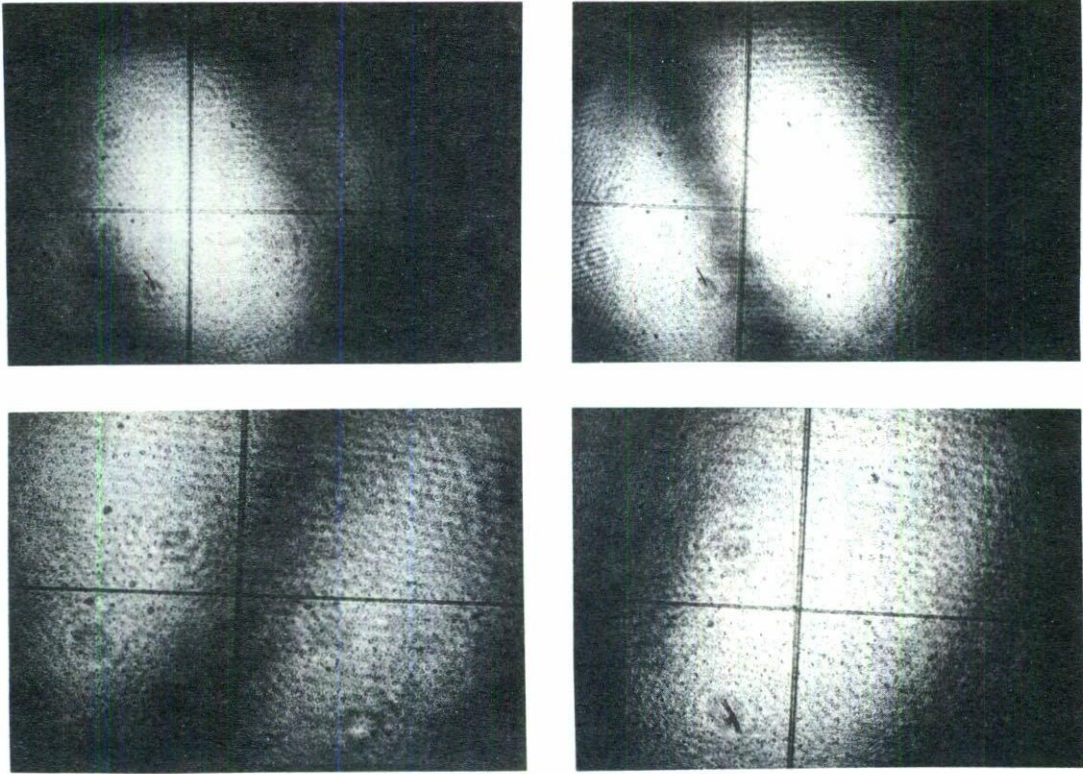
FIGURE 3. Interferograms for $\Theta = 50°$ with nearly equal optical path lengths of both interferometer's arms. Fringes are observed with a very slight deliberate misalignment of beam splitter D_2. Observe the fixed crossline graticule. In Figs. 3a and 3b, photographic plate is at P (symmetrical exit in Fig. 1). From Fig. 3a to Fig. 3b, circular polarization filter at F has been changed from positive to negative. In Figs. 3c and 3d, photographic plate is at P' (asymmetrical exit in Fig. 1). From Fig. 3c to Fig. 3d, circular polarization filter at F' has been changed from positive to negative.

The light at each of the two exits of the interferometer is filtered through a positive (negative) circular polarization filter. This filter was constructed by interposing a compensator $\lambda/4$ quartz plate (Oriel, mod. 25620) (this same plate, preceded by a compensator $\lambda/2$ quartz plate (Oriel, mod. 25670)) to a linear polarizer (Melles-Griot, mod. 03FPG003) with its fast axis at $+45°$ with respect to the transmission axis of the polarizer. As is well known [5], if light runs backwards through this system it gets a state of positive (negative) circular polarization. Running first through the compensator $\lambda/4$ plate ($\lambda/2$ plus $\lambda/4$ compensator plates), and afterwards through the linear polarizer, this system blocks out negative (positive) circular polarization.

Interference fringes produced by filtered photons of positive (negative) helicity are projected over a fixed photographic film together with the image of the crossline reticle used as reference of fringe position. The quantity measured is the relative displacement of interference fringes for photons of opposite helicity obtained when we change the po-
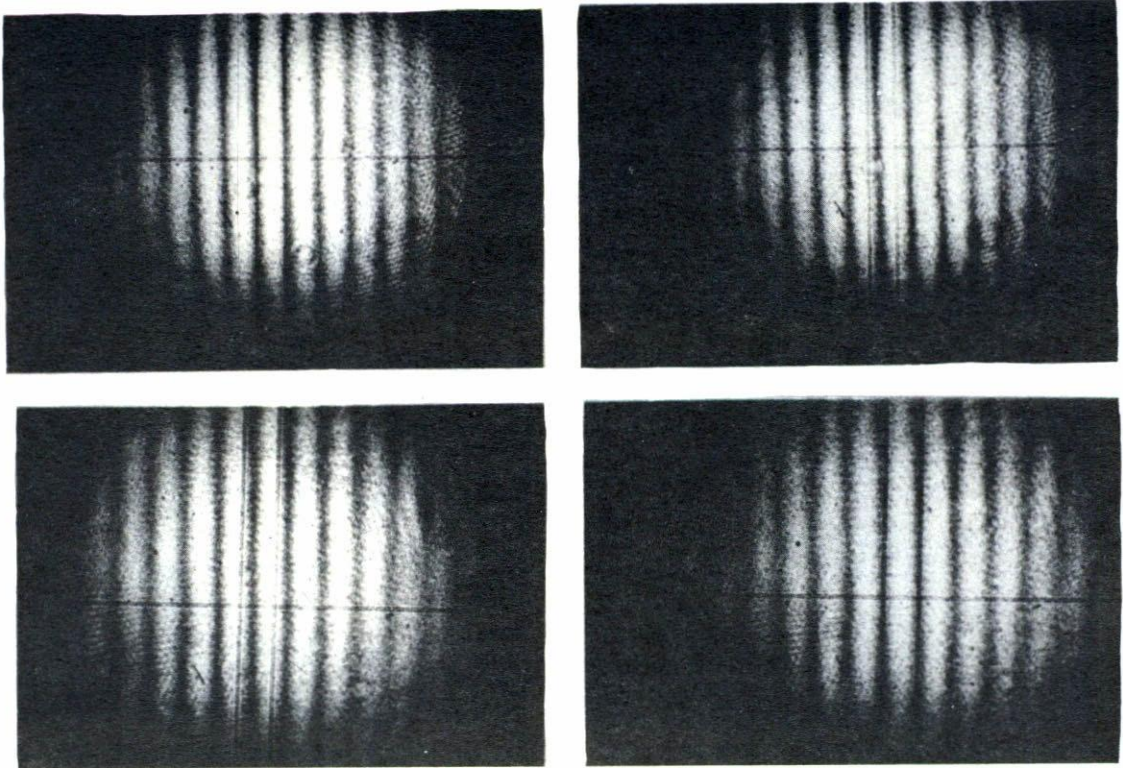
FIGURE 4. Interferograms for $\Theta = 50°$ with an optical flat window added in path β. Fringes are observed with the same misalignment as in Fig. 3. Except for this additional window, photographic plates in Figs. 4a through 4d were exposed in the very same conditions as those in Figs. 3a through 3d, respectively.

sitive circular polarization filter by the negative one. With this set up, we measure the relative displacement of the fringes (mentioned above) as a function of deformation angle Θ (Fig. 1). Results can be interpreted as a manifestation of the geometrical phase for the photon. We do this by means of the following association: In the first hand, the relative displacement of the fringes is related with the geometrical phase shift $\Delta\gamma \equiv \Delta\gamma_- - \Delta\gamma_+$ [see Eq. 3]; in the other hand, the Θ angle in the interferometer arms is related with the total solid angle Ω, where

$$\Omega = \sum_{i,\sigma} \Omega(\mathcal{C}_{i\sigma}). \tag{4}$$

Graphical results are presented in Fig. 5. This verifies the relation of Eq. (1).

We now review the null path length difference repeating criteria. If the difference in the optical path between arms α and β cancels out exactly, we would observe, with the photons travelling in the same homogeneous medium, a unique interference fringe of infinite width
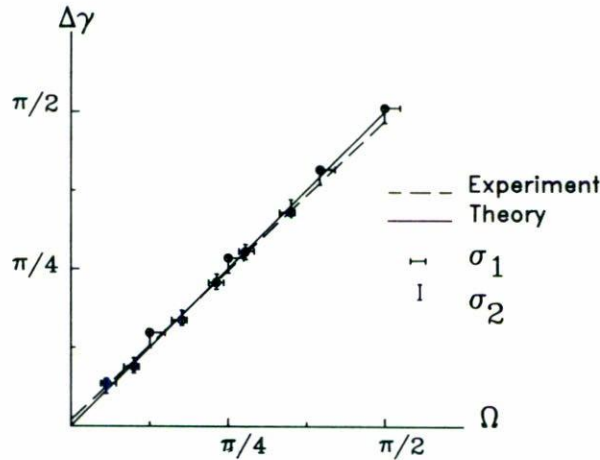
FIGURE 5. Graph of the geometrical phase shift $\Delta\gamma$ vs. the total solid angle Ω.

and radius. Under this circumstances we could also observe interference with white light. Certainly, the deliberate misalignment mentioned above is a tacitly supposed condition to observe a number of fringes and it has not been studied previously in a controlled experiment. In what follows we shall prove experimentally that the relative displacement on the interference fringes corresponding to each helicity is invariant under shifts of the purely dynamical phase.

We add a dynamical phase shift by introducing in one of the arms of the interferometer a homogeneous optical window of flat parallel faces (Ealing, mod. 35-9125), with its normal on the direction of the laser beam. Then we can observe a change in the order of the interference pattern as a reduction in the width and radius of the fringes. However, the relative shift among fringes of opposite helicities remains constant. Figs. 3 and 4 illustrate this.

The present experiment shows that the geometrical phases can manifest not only in the context of non-adiabatical processes, but also in those cases in which the evolution of the state of the system is not strictly cyclic [3]. This takes place if we analyze the interference at the exit port $-Y$, instead of exit port X as we have done (see Fig. 1). In this case the eigenstate of the spin of the photon $|+\rangle$ through the arm α projects the path $ABCD$ over sphere Σ (Fig. 2a) *which is not closed*. Even so, according to the theory of Samuel and Bhandari [3], we can calculate the geometrical phase by closing the circuit with any geodesic going from D to B. We obtained in this way the spherical triangle $ABCD$ on Σ. For the photon $|+\rangle$ through the path β the projective circuit over the sphere Σ is closed. It is, as can be seen easily, the same triangle $ADCBA$ but followed in the opposite sense. If we still consider the exit port $-Y$, for the $|-\rangle$ photon in the α arm we obtain the open path $A'B'C'D'$ (see Fig. 2b). However, as in the previous case, we close this path with the geodesic $D'B'$ to calculate the geometrical phase shift in this arm. With the other arm the same closed circuit $A'D'C'B'$ is projected on Σ, but it is runned on the opposite sense. Then we have that the general situation at the exit port $-Y$ is the same to that one of port X. However, the pattern observed is complementary to that in port

$-X$ because of the reflection *vs.* transmission dynamics, as it would be expected from an energy conservation argument. This is illustrated in Figs. 3 and 4, going from a) and b) to c) and d).

4. CONCLUSION

Projective circuits $C_{i,\sigma}$, of photon spin projected on a unitary sphere Σ, associated with all directions of propagation in configuration space, had to be taken into account in order to include all the fringe shifts observed in the interference pattern of light in the present experiment. In agreement with the Aharonov-Anandan theory, the solid angle subtended by $C_{i\sigma}$ with respect to the center of the sphere Σ gives the magnitude of the geometrical shift.

In this kind of experiments, in contrast with those in which Poincarè sphere represents the projective space, the nature of the fringes itself allow us to identify and measure which proportion, or percentage, of the phase shift is dynamical, and which geometrical. Moreover, in this experiment we proved the statement of the Aharonov-Anandan theory that the geometrical phase is independent of time, of the dynamical phase and of the Hamiltonian; all of which were obviously modified by the introduction of the optical window without affecting the relative position of the fringes of opposite helicity. Finally, in this experiment we also confirm that the requirement of a cyclic evolution of the spin state vector can be relaxed and yet we get geometrical effects.

ACKNOWLEDGEMENTS

REFERENCES

1. M.V. Berry, *Proc. R. Soc. Lond.* **A392** (1984) 45.
2. Y. Aharonov, Anandan, *J. Phys. Rev. Lett.* **58** (1987) 1593.
3. J. Samuel, and R. Bhandari, *J. Phys. Rev. Lett.* **60** (1988) 2339; T.F. Jordan, *J. Math. Phys.* **29** (1988) 2042.
4. R. Bhandari, and J. Samuel, *J. Phys. Rev. Lett.* **60** (1988) 1211; R. Simon, H.J. Kimble, and E.C.G. Sudarshan, *J. Phys. Rev. Lett.* **61** (1988) 19.
5. M. Born and E. Wolf, *Principles of Optics*, Pergamon (1980). Oxford. London. Edinburgh. New York. Paris. Frankfurt.
6. S. Pancharatnam, *Proc. Indian Acad. Sci. Sect.* **A44** (1956) 247; M.V. Berry, *Jour. of Mod. Optics* **34** (1987) 1401.
7. R.Y. Chiao, and Y.S. Wu, *J. Phys. Rev. Lett.* **57** (1986) 933; M.V. Berry, "Interpreting the anholonomy of coiled light", *Nature* **326**, (19 March, 1987) 277.
8. R.Y. Chiao, *et al. J. Phys. Rev. Lett.* **60** (1988) 1214.